

Monte Carlo study of the pairing interaction in the two-leg Hubbard ladder

N. Bulut, T. Dahm and D.J. Scalapino

Department of Physics, University of California

Santa Barbara, CA 93106-9530

Abstract

Monte Carlo calculations of the irreducible particle-particle interaction on a two-leg Hubbard ladder doped near half-filling are reported. As the temperature is lowered, this interaction develops structure in momentum space similar to the magnetic susceptibility $\chi(\mathbf{q})$ and reflects the development of strong short-range antiferromagnetic correlations. Using this interaction, the eigenfunction of the leading singlet pair eigenvalue is found to have $d_{x^2-y^2}$ like symmetry. The single-particle spectral weight is also shown to peak near $(\pi, 0)$ and $(0, \pi)$ when the ratio of the inter- to intra-chain hopping $t_{\perp}/t \simeq 1.5$, leading to an increased tendency for pairing.

Numerical calculations, renormalization-group bosonization studies as well as strong-coupling treatments find that half-filled t - J or Hubbard two-leg ladders have a spin gapped ground state with short range antiferromagnetic correlations [1–3]. Furthermore, these various techniques all find that when holes are doped into the ladder, $d_{x^2-y^2}$ -like pairing correlations develop. This being the case, one would like to understand the nature of the effective interaction that gives rise to the $d_{x^2-y^2}$ pairing correlations for this system. Here, in order to address this question, we present Monte Carlo results for the irreducible particle-particle interaction Γ_I . In addition, we use Γ_I and the single-particle Green's function obtained from the Monte Carlo calculations to solve the Bethe-Salpeter equation in the singlet pairing channel. We find that the eigenfunction with the leading eigenvalue has $d_{x^2-y^2}$ -like symmetry.

The Hubbard model Hamiltonian for a two-leg ladder has the form

$$H = -t \sum_{i,\lambda,s} (c_{i\lambda s}^\dagger c_{i+1\lambda s} + \text{h.c.}) - t_\perp \sum_{i,s} (c_{i1s}^\dagger c_{i2s} + \text{h.c.}) + U \sum_{i\lambda} n_{i\lambda\uparrow} n_{i\lambda\downarrow}. \quad (1)$$

Here t is the intra-chain one electron hopping, t_\perp the inter-chain hopping and U the on-site Coulomb interaction. The operators $c_{i\lambda s}^\dagger$ and $c_{i\lambda s}$ create and destroy electrons of spin s on site i of the λ^{th} leg, respectively, and $n_{i\lambda s} = c_{i\lambda s}^\dagger c_{i\lambda s}$ is the occupation number for spin s on site i of the λ^{th} leg.

Using Monte Carlo techniques, we have calculated the finite temperature two-particle Green's function

$$G_2(x_4, x_3, x_2, x_1) = -\langle T c_\uparrow(x_4) c_\downarrow(x_3) c_\downarrow^\dagger(x_2) c_\uparrow^\dagger(x_1) \rangle. \quad (2)$$

Here $c_s^\dagger(x_i)$ with $x_i = (\mathbf{x}_i, \tau_i)$ creates an electron of spin s at site \mathbf{x}_i and imaginary time τ_i and T is the usual τ -ordering operator. Then, as previously discussed [4], one can take the Fourier transform of both the space and imaginary time variables and obtain $G_2(p', k', k, p)$ with $p' = (\mathbf{p}', i\omega_n)$, etc. This two particle Green's function can be expressed in terms of the exact single-particle propagator $G_s(\mathbf{p}, i\omega_n)$ and the reducible particle-particle vertex $\Gamma(p', k', k, p)$

$$\begin{aligned}
G_2(p', k', k, p) = & -\delta_{p,p'} \delta_{k,k'} G_{\downarrow}(k) G_{\uparrow}(p) \\
& + \frac{T}{N} \delta_{p'+k', p+k} G_{\uparrow}(p') G_{\downarrow}(k') \Gamma(p', k', k, p) G_{\downarrow}(k) G_{\uparrow}(p).
\end{aligned} \tag{3}$$

Then from the Monte Carlo data for G and G_2 , one can determine $\Gamma(p', k', k, p)$. Finally, because the effective pairing interaction corresponds to the irreducible particle-particle interaction Γ_I in the zero energy and momentum center of mass channel, we have inverted the fully dressed t -matrix equation to find Γ_I in terms of Γ and G . Setting $k = -p$ and $k' = -p'$, the fully dressed t -matrix equation becomes

$$\Gamma(p'|p) = \Gamma_I(p'|p) - \frac{T}{N} \sum_k \Gamma(p'|k) G_{\downarrow}(-k) G_{\uparrow}(k) \Gamma_I(k|p), \tag{4}$$

which is solved to find $\Gamma_I(p'|p)$. The effective pairing interaction in the singlet channel is

$$V(p' - p) = \frac{1}{2} (\Gamma_I(p'|p) + \Gamma_I(-p'|p)). \tag{5}$$

We have carried out this calculation at different temperatures for various values of the hopping anisotropy t_{\perp}/t , interaction strength U/t and filling $\langle n \rangle = \langle n_{i\uparrow} + n_{i\downarrow} \rangle$. Here, we will show results for $t_{\perp}/t = 1.5$, $U/t = 4$, $\langle n \rangle = 0.875$ and a 2×16 lattice. We have chosen this set of parameters, because the numerical density matrix renormalization group (DMRG) calculations find that for $U/t = 4$ and $\langle n \rangle = 0.875$, the $d_{x^2-y^2}$ pairing correlations are strongest when $t_{\perp}/t \simeq 1.5$ [5]. In addition, for these parameters we have good control of the maximum entropy analytic continuation of the Monte Carlo data, which is necessary to obtain the single-particle spectral weight $A(\mathbf{p}, \omega)$.

In Fig. 1 we plot the effective pairing interaction V versus $q_x = p'_x - p_x$ for $q_y = p'_y - p_y = \pi$. Here we have set $\omega_n = \omega_{n'} = \pi T$ corresponding to $\omega_m = 0$ energy transfer. The three curves correspond to temperatures $T = 1.0t$, $0.5t$ and $0.25t$. One can see that as the temperature decreases, the effective pairing interaction becomes increasingly positive at large momentum transfer $\mathbf{q} \rightarrow (\pi, \pi)$. As shown in Figure 2, the magnetic susceptibility

$$\chi(\mathbf{q}) = \frac{1}{N} \int_0^{\beta} d\tau \sum_{\ell} e^{i\mathbf{q}\cdot\ell} \langle m_{i+\ell}^-(\tau) m_i^+(0) \rangle \tag{6}$$

also develops structure at large momentum transfers over this same temperature region. Thus it is clear that the effective pairing interaction is associated with the development of short-range antiferromagnetic correlations.

It is also of interest to study the Bethe-Salpeter equation for the singlet particle-particle channel

$$\lambda_\alpha \phi_\alpha(\mathbf{p}, i\omega_n) = -\frac{T}{N} \sum_{\mathbf{p}', i\omega_{n'}} \Gamma_I(\mathbf{p}, i\omega_n | \mathbf{p}', i\omega_{n'}) |G(\mathbf{p}', i\omega_{n'})|^2 \phi_\alpha(\mathbf{p}', i\omega_{n'}). \quad (7)$$

Fig. 3 shows the eigenfunction $\phi(\mathbf{p}, i\omega_n)$ of the leading eigenvalue versus \mathbf{p} for $\omega_n = \pi T$. We observe that $\phi(\mathbf{p}, i\pi T)$ has $d_{x^2-y^2}$ -like momentum structure in the sense that it has opposite signs and is largest near $(\pi, 0)$ on the bonding band and near $(0, \pi)$ on the antibonding band. This is associated with the structure of the irreducible interaction Γ_I and the single-particle spectral weight $A(\mathbf{p}, \omega)$ which we will study below [6].

The temperature dependence of the leading eigenvalue λ_1 is plotted in Fig. 4(a). As previously discussed, when the temperature is lowered, short-range antiferromagnetic correlations develop and the effective pairing interaction increases at large momentum transfer. This leads to an increase in λ_1 as shown in Fig. 4(a). We believe that λ_1 will approach unity at low temperatures where power-law $d_{x^2-y^2}$ -like pairing correlations have been shown to exist using density matrix renormalization group techniques [2]. In Fig. 4(b), we show the dependence of the leading eigenvalue λ_1 on the hopping anisotropy t_\perp/t . According to the DMRG calculations [5], for $U/t = 4$ and $\langle n \rangle = 0.875$ the pairing correlations in the ground state are strongest when $t_\perp/t \simeq 1.5$. In Fig. 4(b), we do not observe a strong dependence of λ_1 on t_\perp/t because of the thermal smearing effects at $T = 0.25t$.

In addition to the irreducible interaction vertex Γ_I , the single-particle Green's function $G(\mathbf{p}, i\omega_n)$ is also important in determining the structure of the leading eigenfunction of the Bethe-Salpeter equation. Using a numerical maximum entropy procedure [7], we have calculated the single-particle spectral weight

$$A(\mathbf{p}, \omega) = -\frac{1}{\pi} \text{Im} G(\mathbf{p}, \omega). \quad (8)$$

This is plotted in Fig. 5 for $t_{\perp}/t = 1.5$ as a function of ω for different \mathbf{p} . Here, the solid curves are for the bonding band ($p_y = 0$) and the dotted curves are for the antibonding band ($p_y = \pi$). We see that for this value of t_{\perp}/t , the bonding band has spectral weight near the Fermi level for $\mathbf{p} \sim (\pi, 0)$, and the antibonding band has spectral weight near the Fermi level for $\mathbf{p} \sim (0, \pi)$. Hence, these Fermi points can be connected by scatterings involving $\mathbf{q} = (\pi, \pi)$ momentum transfer. Since Γ_{IS} is large and repulsive for $\mathbf{q} \sim (\pi, \pi)$, the leading eigenfunction ϕ of the Bethe-Salpeter equation has opposite signs for \mathbf{p} near $\mathbf{p} = (\pi, 0)$ and $(0, \pi)$, as seen in Fig. 3.

These calculations provide further insight into the structure of the effective pairing interaction and the single-particle spectral weight which lead to the pairing correlations in the two-leg Hubbard ladder. Specifically, the momentum structure of the effective interaction $V(\mathbf{q})$ clearly reflects the existence of short-range antiferromagnetic correlations as the cause of the increasing positive strength of $V(\mathbf{q})$ at large momentum transfer. Secondly, the enhanced spectral weight in the bonding band near $(\pi, 0)$ and the antibonding band near $(0, \pi)$ are reminiscent of a similar effect observed in the two-dimensional Hubbard model near half-filling [8,9] and in the ARPES of the cuprates [10]. This enhanced low lying spectral weight associated with the renormalized quasiparticles is such that pair scattering processes with momentum transfers near (π, π) have increased phase space. These two features appear to play an important role in the development of pairing on the two-leg ladder, just as they do for the two-dimensional Hubbard model.

ACKNOWLEDGMENTS

The authors gratefully acknowledge support from the National Science Foundation under Grant No. DMR95-27304, DMR95-20636 and PHY94-07194, and from the Deutsche Forschungsgemeinschaft. The numerical computations reported in this paper were performed at the San Diego Supercomputer Center.

REFERENCES

- [1] T.M. Rice, S. Gopalan and M. Sigrist, *Europhys. Lett.* **23**, 445 (1993); H. Tsunetsugu, M. Troyer and T.M. Rice, *Phys. Rev. B* **49**, 16078 (1994).
- [2] R.M. Noack, S.R. White and D.J. Scalapino, *Phys. Rev. Lett.* **73**, 882 (1994); *Physica C* **270**, 281 (1996).
- [3] L. Balents and M.P.A. Fisher, *Phys. Rev. B* **53**, 12133 (1996).
- [4] N. Bulut, D.J. Scalapino and S.R. White, *Phys. Rev. B* **47**, 2742 (1993).
- [5] R.M. Noack, N. Bulut, D.J. Scalapino and M.G. Zacher, preprint.
- [6] We note that as t_{\perp}/t is varied, the momentum structure of the single-particle spectral weight and the irreducible interaction changes. Consequently, the momentum structure of the leading eigenfunction ϕ changes. A discussion of how ϕ is affected by t_{\perp}/t and further results on the doping dependence will be given in a longer article. Here, we concentrate on a set of parameters for which the DMRG calculations find enhanced pairing correlations.
- [7] S.R. White, *Phys. Rev. B* **44**, 4670 (1991).
- [8] N. Bulut, D.J. Scalapino and S.R. White, *Phys. Rev. B* **50**, 7215 (1994).
- [9] R. Preuss, W. Hanke and W. von der Linden, *Phys. Rev. Lett.* **75**, 1344 (1995).
- [10] For a review, see Z.-X. Shen and D.S. Dessau, *Physics Reports* **253**, 1 (1995).

FIGURES

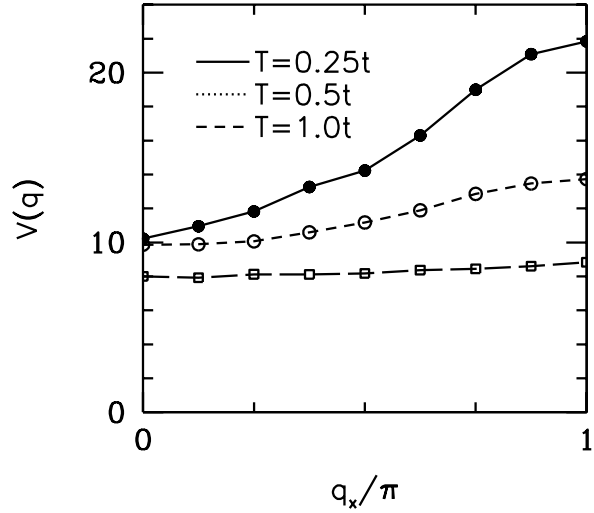


FIG. 1. Momentum dependence of the effective interaction $V(\mathbf{q})$ for $U = 4t$, $\langle n \rangle = 0.875$ and $t_{\perp} = 1.5t$. Here $V(\mathbf{q})$ is measured in units of t , $q_y = \pi$ and $V(\mathbf{q})$ is plotted as a function of q_x .

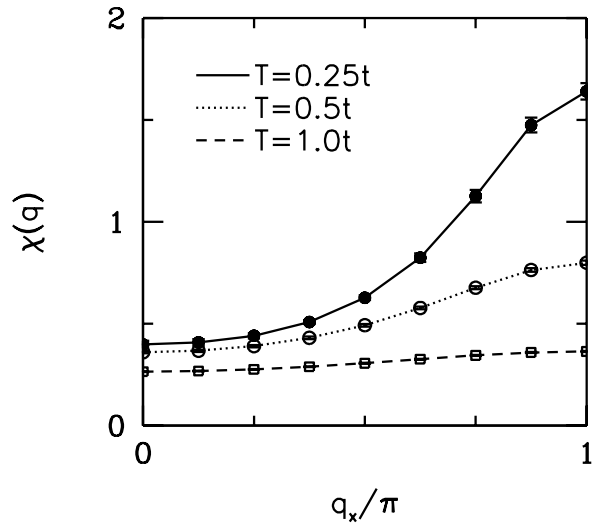


FIG. 2. Momentum dependence of the magnetic susceptibility $\chi(\mathbf{q})$ for $U = 4t$, $\langle n \rangle = 0.875$ and $t_{\perp} = 1.5t$. Here $q_y = \pi$ and $\chi(\mathbf{q})$ is plotted as a function of q_x .

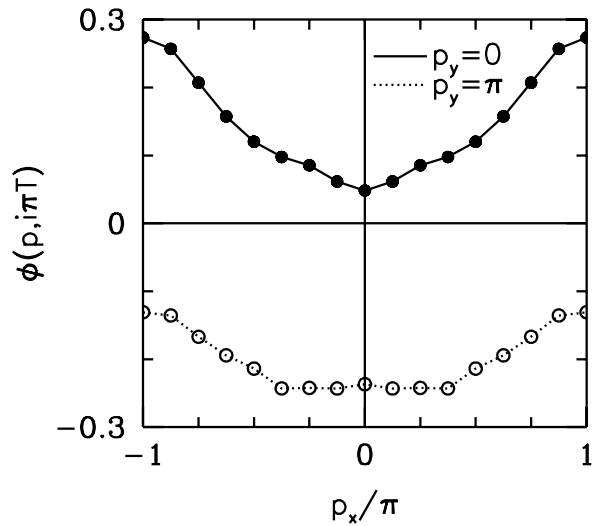


FIG. 3. Momentum dependence of the $d_{x^2-y^2}$ eigenfunction $\phi(\mathbf{p}, i\pi T)$. These results are for $T = 0.25t$, $U = 4t$, $\langle n \rangle = 0.875$ and $t_\perp = 1.5t$.

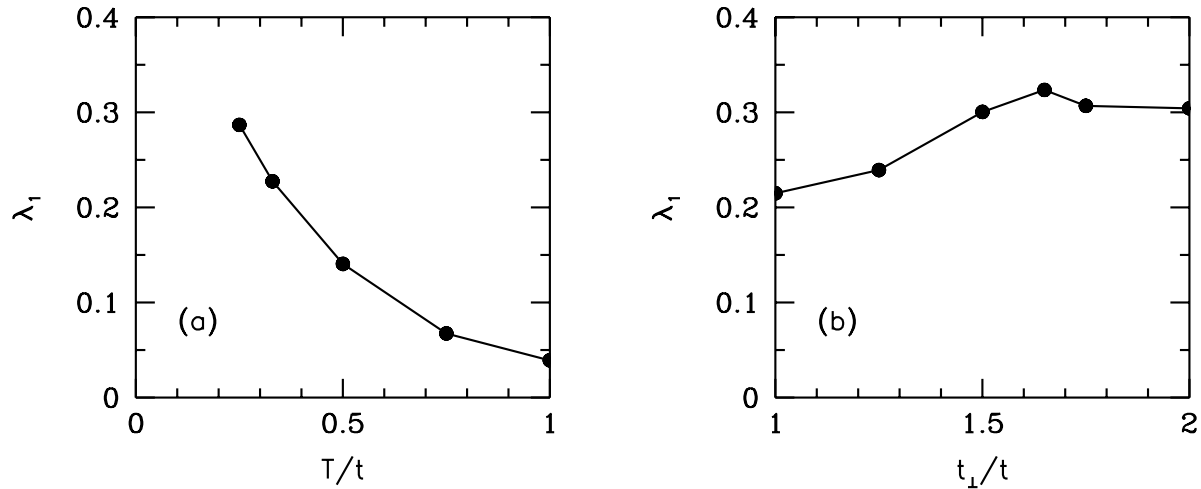


FIG. 4. (a) Temperature dependence of the leading eigenvalue λ_1 for $t_\perp = 1.5t$. (b) λ_1 vs t_\perp/t for $T = 0.25t$. These results are for $\langle n \rangle = 0.875$ and $U = 4t$.

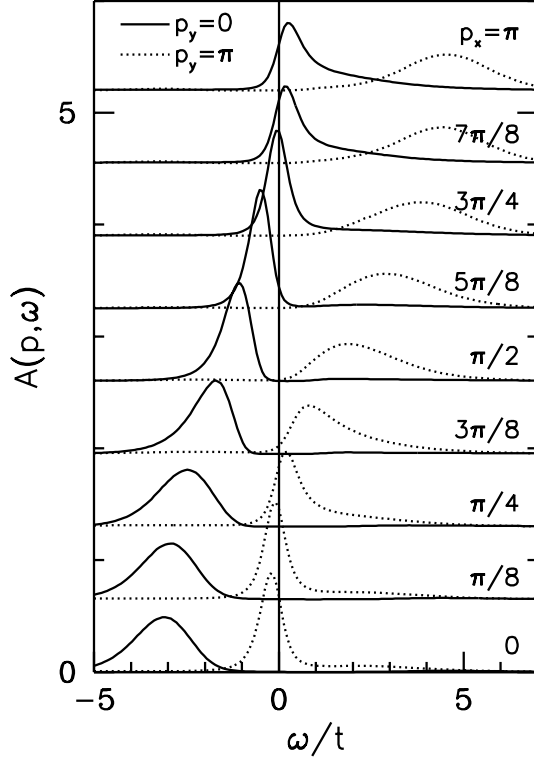


FIG. 5. Single-particle spectral weight $A(\mathbf{p}, \omega)$ versus ω for $t_{\perp}/t = 1.5$, $T = 0.25t$, $U/t = 4$ and $\langle n \rangle = 0.875$. The solid curves denote the results for the bonding band ($p_y = 0$) and the dotted curves denote the results for the antibonding band ($p_y = \pi$).